DESIGN METHOD OF FABRIC FORMED CONCRETE BEAMS REINFORCED WITH W-FRP

Yuanzhang YANG[1], Jiangpeng Shu[2], Weijian Zhao[2], John ORR[3], Tim IBELL[4]

1. Postdoctoral Researcher, College of Civil Engineering and Architecture Zhejiang University, Hangzhou, China
2. Professor, College of Civil Engineering and Architecture Zhejiang University, Hangzhou, China
3. Lecturer, Department of Civil Engineering, University of Cambridge, Cambridge, UK
4. Professor, Department of Architectural and Civil Engineering, University of Bath, Bath, UK

Corresponding author email: yy701@zju.edu.cn

Abstract

Flexible moulds as external formwork and a novel robotically fabricated reinforcement, Wound FRP (W-FRP), provide the solution for the manufacture of complex structural concrete components being optimised to minimise material use and further reduce the carbon emissions from constructional industry. However, previous research has shown that the non-prismatic geometries and linear-elastic reinforcement could result in very different structural behaviours from the traditional concrete beams and invalidity of the existing codified design approaches. This research proposes revisions to the empirical equation to calculate the tensile force of inclined flexural reinforcement and a design method to predict the shear capacity of the W-FRP reinforced non-prismatic beams based on Modified Compression Field Theory (MCFT). A full-scale test of fabric formed T beam reinforced with W-FRP was conducted to demonstrate the validity of this new design approach. The research in this paper shows that: 1) the invalidity of the codified design approach could be attributed to the empirical calibration with prismatic beams; 2) geometry of the beam and the W-FRP shear reinforcement ratio are the main factors influence the flexural bar force development and 3) the proposed equation for calculating tensile force of flexural reinforcement could accurately predict the force development. This research provides a practical and valid approach for the future design of non-prismatic beams reinforced with W-FRP and addresses technical challenges in the way to minimising material use in concrete structures.

Keywords: *Fabric formwork, W-FRP, MCFT, Structural behaviour.*

1. Introduction

Fabric formwork (Veenendaal*, et al.*, 2011) is a mould system using woven fabrics to shape wet concrete and it has shown great advantages to build non-prismatic concrete structural element with low cost. However, due to the variable depth geometry, reinforcement cage fabrication is complicated requiring high labour and time cost (Orr, 2012). Wound-Fibre-Reinforced-Polymer (Spadea*, et al.*, 2017) is fabricated by winding wet continuous carbon fibre tows coated with epoxy resin around a mandrel composed of flexural bars. The W-FRP shear links can automatically adapt to the variable-depth beam geometry and has been successfully used in concrete beams with both prismatic and non-prismatic geometries (Spadea*, et al.*, 2017, Yang*, et al.*, 2018).

Although optimised concrete structures could be constructed with ease capitalising on the fabric formwork and W-FRP reinforcement, there has been no explicit codified design method for designers. Previous experimental research (Yang*, et al.*, 2017) has shown that due to the linear-elastic reinforcement and non-prismatic geometries, fabric formed beams reinforced with W-FRP have different structural behaviours compared to conventional steel reinforced prismatic beams.

With the shallower support depth of fabric formed beams, in addition to the flexural tensile force, an additional tensile force (Paglietti and Carta, 2009) due to shear action also develops in the flexural bars. This tensile force can provide a certain amount of shear contributions but could also result in potential premature anchorage failure. Although many design codes and guidelines (BSI, 2004, CSA, 2012) have already addressed the additional tensile force and provided empirical equations to calculate the

additional tensile force and corresponding shear contribution, it was found in our previous research (Yang, *et al.*, 2017) that the codified empirical equations greatly underestimate the bar force of inclined longitudinal reinforcement as the equations were calibrated with conventional prismatic beams and the equations cannot provide a full loading process simulation of the longitudinal bar force. Consequently, the shear capacity of fabric formed beams reinforced with W-FRP cannot be accurately predicted and the required anchorage strength cannot be determined.

To address the shear design and anchorage design issue, this paper proposes revisions for the existing empirical equations to calculate the incline flexural bar force and formulates a new design approach based on Modified Compression Field Theory (MCFT) (Vecchio and Collins, 1986) for fabric formed beams and previous experimental research of fabric-formed T beams reinforced with W-FRP reinforcement. A new T beam design was proposed for the previous experimental research and tested to demonstrate the validity of the proposed revisions and design method.

2. Previous Experimental research

Our previous experimental research investigated the structural behaviours of W-FRP reinforced T beams reinforced with non-prismatic geometries (Yang, *et al.*, 2017). The experimental campaign included 11 beams, which were designed based on CSA S806 (2012). All the beams had the same length of 4m, a clear span of 3m, mid-span depth of 250mm, mid-span web width of 100mm, and support web width of 200mm and were tested under seven-point bending to simulate uniformly distributed load as shown in Figure 1. Three different support depths (120mm, 180mm and 110mm) were chosen to investigate the influence of geometry. Five types of anchorage (with or without splayed anchorage) were designed to understand the influence of anchorage strength. All specimens had different shear reinforcement layouts. The design details and test results are summarised in Table 1.

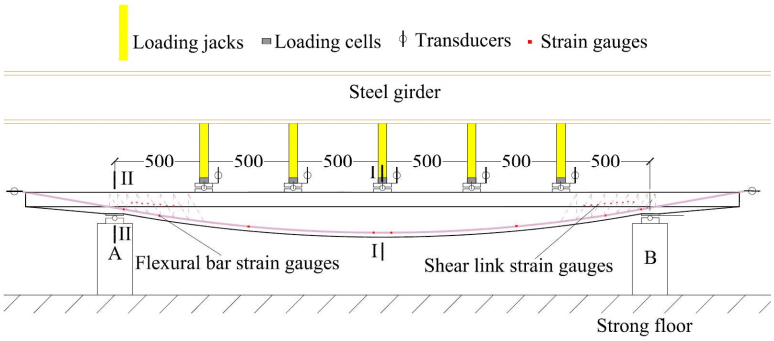

Figure 1 Test setup and instrumentation

Table 1 Design details and test results summation of specimens

Specimen	Support depth (mm)	Shear design			Anchorage type	Predicted failure load (kN) by CSA S806 (and mode)	Actual failure load (kN) (and mode)
		Shear reinforcement ratio ρ_{fv} (%)	Angles of shear links α_1/α_2 (°)	Cross section area A_{fv} (mm^2)			
T1	A(120)	-	-	-	II	47 (S)	101(S)
T2-1	A(120)	0.34	60/90	8.6	I	200 (S)	153(ES)
T2-2	A(120)	0.34	60/90	4.3	I	200 (S)	160(ES)
T2-1R	A(120)	0.34	60/90	8.6	III	200 (S)	188(S)
T2-2R	A(120)	0.34	60/90	4.3	III	200 (S)	222(ES)
T3-1	A(120)	0.34	45/65	5.6	II	200 (S)	226(ES)

T3-2	A(120)	0.34	45/65	4.3	II	200 (S)	253(F)
T4-1	B(180)	0.64	45/65	21.4	IV	258 (F)	279(F)
T4-2	B(180)	0.26	45/65	8.6	V	199 (S)	217(ES)
T5	A(120)	0.85	45/65	21.4	IV	258 (F)	261(F)
T6	C(110)	0.87	45/65	21.4	V	258 (F)	233(F)

Note: 1. the anchorage types are detailed in our previous work
2. S denotes shear failure, ES denotes end-slip failure and F denotes flexural failure.

It was highlighted that except for specimen T1 and T2-1R failing in shear, the remaining specimens designed for shear failure encountered an unexpected type of end-slip failure mode with flexural bars being pulled into the concrete flange. All these specimens failed in end-slip encountered shear link rupturing and there were load redistributions from shear links to flexural reinforcement as shown in Figure 2, where T_{vv} is the shear contribution from shear links in the shear span and T_{fv} is the vertical component of flexural bar force at the support. Finally, most of the shear links in the shear span of the end-slip failure specimens ruptured and failed in end-slip due to the large tensile force developed in the flexural bars.

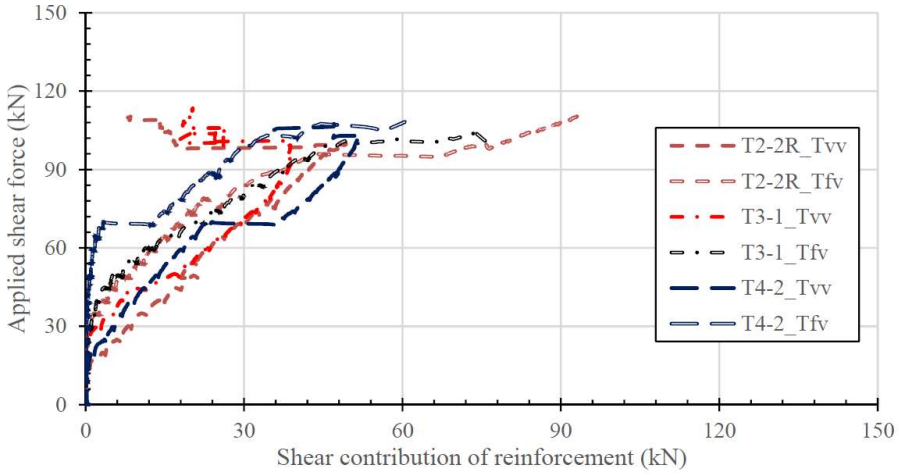

Figure 2. Shear contribution of flexural and shear reinforcement in specimens T2-2R, T3-1 and T4-2

The unexpected end-slip failure could be attributed to the underestimation of flexural bar force following the codified design, which was mainly caused by the empirical method used to formulate equations in the codes. CSA S806 (2012) uses a constant 1.3 to describe the cotangent of the angle of the concrete strut, assuming this angle to be approximately 52 degrees. However, due to the variable-depth geometry, if assuming the tangent of concrete strut angle as $M_a/(V_a d)$, the concrete strut angle of the specimens could reach as low as 13 degrees, which would cause a great difference in the codified prediction.

In addition, the design following CSA S806 (2012) does not consider the rotation of the support, which was observed in the testing. When the inclined flexural bar is considered to provide shear contributions, the calculations of the bar force and its vertical component are sensitive to the slope of flexural bars. The displacement of the specimens resulted in rotation of the supports and the angles of the concrete strut and flexural bars to the horizontal axis changed accordingly, which could significantly increase the flexural bar force and its vertical component.

As no load redistribution from W-FRP shear links to flexural CFRP bars can be considered following CSA S806 (2012), the beams which encountered end-slip failure cannot be predicted. Without understanding the flexural bar force in the full loading process, no required anchorage strength could be provided. Therefore, a new approach involving further revisions to the existing design approach is required to accurately predict the bar force of inclined flexural reinforcement, correct failure mode and ultimate capacity.

3. Proposed design method

3.1. Additional tensile force

The basic philosophy behind the empirical equations from different design codes and guidelines is to take moment about the loading point in the free body, which is cut from the loading point to the support, as shown in Figure 3. By taking moments about Point A, the tensile force in the longitudinal bars near the support can be calculated with Equation 1

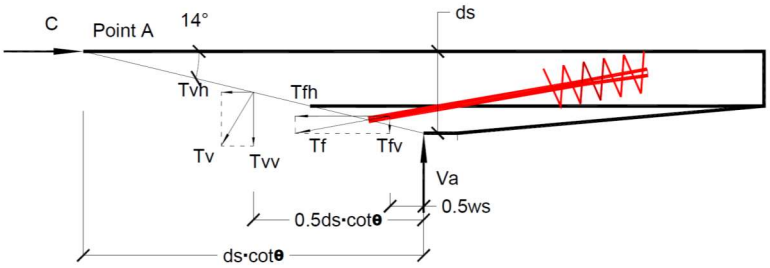

Figure 3 Equilibrium of free body of tested specimens at the support area

$$T_f = \frac{\left(V_a - \frac{T_{vv}}{2}\right) cot\,\theta - T_{vh}/2}{(1 + tan\,\beta\, cot\,\theta)\, cos\,\beta} \tag{1}$$

In Equation 4, the shear force due to the aggregate interlock along with the diagonal cut is assumed to have the same direction with the cut and T_f and V_a is assumed to have the same location. Therefore, both of the parts can be neglected. As W-FRP could be fabricated into different forms, which incorporate diagonal links, the influence of shear link direction is considered by T_{vh} and T_{vv}. The non-prismatic geometry is considered by incorporating the angle of concrete strut θ and flexural reinforcement β. To consider the support rotation (Figure 3), the same equation is used whilst the values of θ and β are set as the actual angles to the horizontal axis rather than the values shown in the design. This requires accurate prediction of the load-deflection relation. The equivalent moment of inertia method developed by Bischoff was adopted for stiffness calculation.

3.2. Flexural bar force and shear capacity calculation based on MCFT

As codified equations of shear design and flexural bar force calculation cannot provide the full-loading process simulation, Modified Compression Field Theory (MCFT) (Vecchio and Collins, 1986) is adopted to calculate the shear capacity. MCFT is considered as an effective design and analysis method for FRP reinforced concrete beams by combining stress equilibrium, strain compatibility, constitutive relations and cracking behaviours (Bentz*, et al.*, 2006). It also has shown good validity for calculating the shear capacity of beams with non-prismatic geometries (Yang*, et al.*, 2018). The inclined flexural bar force and shear capacities of the tested specimens could be calculated with the following procedures:

1. Divide the full loading process into various loading steps. For each loading step, calculate the loading action (such as applied bending moment M_a and shear force M_a) at the critical section and the beam displacement at the loading point. For the tested specimens, the critical section is chosen as the edge of the support plate.
2. Calculate the horizontal normal strain ϵ_n and shear stress v_a at the mid-depth of the critical cross section as the initial input for MCFT calculation. The shear contribution of flexural reinforcement is excluded at this step.
3. Conduct MCFT calculation to obtain the stress and strain state of the shear links and Compare the strain of W-FRP shear links ϵ_{fv} to the design strain of W-FRP links ϵ_{fb}. Where ϵ_{fv} is lower than ϵ_{fb}, use the applied shear stress v_a and the section property to calculate the shear capacity provided by the critical section F_v. Otherwise, F_v is regarded as zero and output shear failure.
4. Calculate the flexural bar force T_f with Equation 4 and its vertical component T_v with the calculated displacement data of loading point.

5. Calculate the total shear resistance V_u as F_v+T_v. Where the difference between V_u and V_a (D) is larger than a specified error limit, recalculate the value of v_a by reducing the shear resistance of flexural bars T_v from the applied shear force V_a.
6. Iterate from step 2 under the D is lower than the error range. Output F_v and T_v.
7. Repeat the calculation for each loading step.

4. Parametric analysis and proposed design case

Following the proposed approach, the bar force development of incline flexural reinforcement and its shear contribution could be calculated. Parametric analysis was conducted to investigate the influence of major design factors of previous experimental research on the bar force development and corresponding shear contribution. The geometry and shear reinforcement ratio were considered.

The parametric analysis of the geometries was conducted with varying profiles of beam bottoms by changing the support depth from 80mm (the depth of flange of the T beams) to 250mm (mid-span depth). A design case with support depth of 110mm is added to demonstrate the minimum support depth with flexural failure occurring at the mid-span and without compromising the flexural capacity. The same material properties of the previous testing were adopted. The average tensile strains of the flexural bars at the support area are plotted against total applied load as shown in Figure 4. It shows that with increasing support depth, both the flexural bar strains and the corresponding shear contributions decrease due to the larger angle of the concrete strut and flexural bars to the horizontal axis.

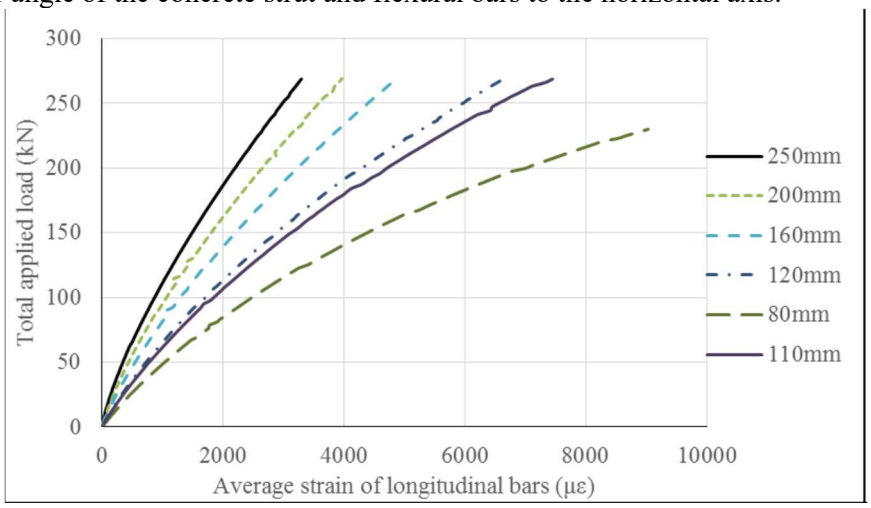

Figure 4. Tensile strains of flexural reinforcement with varying support depth

The shear contributions of the flexural bars and comparisons to the applied shear force are shown in Table 2. For the design case with support depth 110mm, which minimizes the concrete usage without compromising the flexural capacity, the average strain of flexural bars reaches 0.74%. As in the previous experimental results, the flexural bars will not encounter end-slip failure with 0.74% developed strain when no splayed anchorage was installed. Therefore, no additional anchorage is expected for this design case.

Table 2. Comparisons of shear contributions to the applied shear force of design cases with varying support depth

Support depth (mm)	Shear contributions of flexural bars Tv (kN)	Applied shear force at ultimate capacity Va(kN)	Tv/Va
250	8.2	135	0.06
200	18.7	135	0.14
160	31.7	135	0.24
120	55.6	135	0.41
80	88.3	116	0.77

110	65.8	135	0.49

The parametric analysis of shear reinforcement amount is also conducted based on the model of the design case with support depth of 110mm. It is assumed that after the shear link rupture, the flexural bars will carry all the applied shear force as observed in the testing. In the modelling, the shear reinforcement ratio increases from 0.3% at increments of 0.03% until no rupture of shear links can be found.

The analysis results are shown in Figure 5. The flexural bars carry higher strains along with the increasing load. Whilst the shear reinforcement ratio is set below 0.39%, there are platforms of the curves, indicating that the shear links are ruptured and all the applied shear force used to be carried by shear links is transferred to the flexural bars. As long as the anchorage is secured, the strain of the flexural bars will continue to grow until the load of flexural failure. When the shear reinforcement reaches or over 0.39%, the shear links will not rupture and the design case will fail in flexure at the mid-span. The tensile strain of flexural bars will be limited to 0.74%, which provides 65.8kN vertical shear contribution, accounting for 0.49 of the total applied force (Table 2).

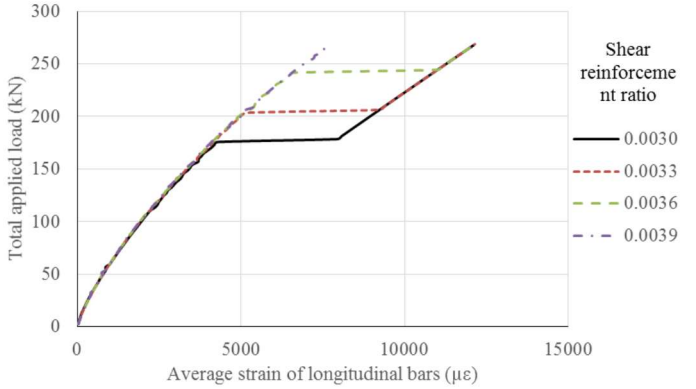

Figure 5. Tensile strain of flexural bars with varying shear reinforcement ratio

Following the parametric analysis results of geometry and shear reinforcement ratio, an optimal design case for the tested specimens is proposed, which consume the least of concrete and shear reinforcement without compromising the structural behaviours. The optimal design case has a support depth of 110mm and mid-span depth of 250mm. The shear reinforcement pattern of specimen T3-2 is used. By increasing the shear reinforcement ratio to over 0.39%, the design case is predicted to fail in flexure at a total applied load of 271kN at the mid-span without shear link rupture and end-slip of flexural bars.

5. Test examination

To verify the validity of the modelling and parametric analysis results, an additional specimen (T7) was constructed following the design details of the optimal case and tested with the same test setup of previous specimens. As expected, specimen T7 failed in flexure at 245kN due to flexural bar rupturing (Figure 6) without end-slip being found. The test results of deflection and the average strain of flexural bars at the support area are plotted against load and compared with the predictions in Figure 7 and Figure 8, respectively.

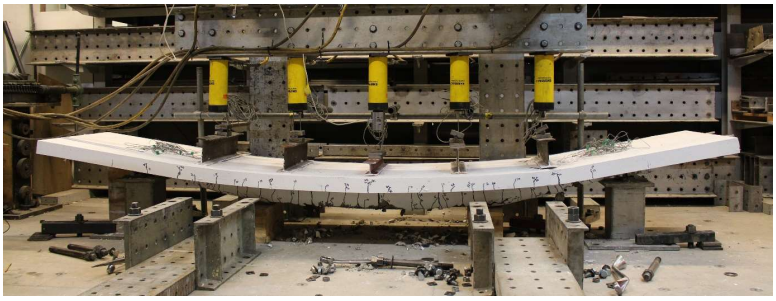

Figure 6. Flexural failure of specimen T7

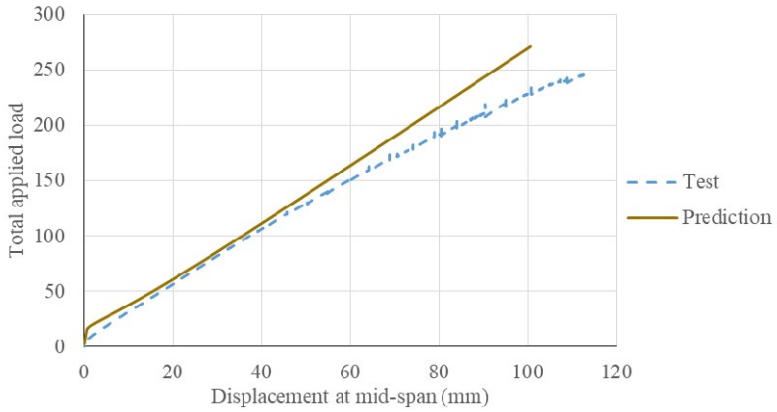

Figure 7. Load-deflection curves of test and prediction

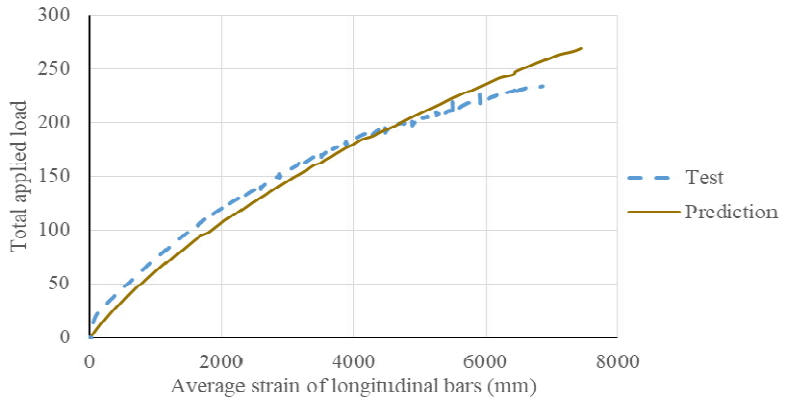

Figure 8. Load-strain curves of flexural bars at the supports of test and prediction

The prediction (271kN) overestimate the flexural capacity by approximately 10%, which could be attributed to the variations of the strength of flexural bars. The prediction model also tends to slightly underestimate the bar strain after approximately 200kN of total applied load. The flexural bar strain in test reached 0.7%, 7% higher than the prediction (0.65%) at the same load. This underestimation could be caused by the inaccurate prediction of load-deflection relation (Figure 7) and the fact that there were a few shear links found ruptured whilst the prediction model cannot simulate the gradual rupturing of single shear links.

Although the limited differences between test results and predictions were found, it can be concluded that the prediction model shows good validity to predict the ultimate capacity, stiffness and development of tensile force in flexural bars. Further improvement could be achieved by using a more accurate approach to predict the load-deflection relation and method which can simulate the gradual rupturing of W-FRP links.

6. Conclusions

This paper presents a new design approach developed based on previous experimental research and MCFT to address the underestimation of bar force of inclined flexural reinforcement of simply supported fabric formed beams by codified empirical design approach. Following the parametric analysis of the previous experimental research based on the new design approach, an optimal design case was proposed and tested. The research supports the following conclusions:

1. The underestimation of flexural bar force by codified method could be attributed to the empirical simplification for prismatic beams: constant angle of the concrete strut and omitted influence of deflection.

2. The geometry influences the shear performance of the beams by varying the shear contribution of flexural bars. With low support depth (80mm), the shear contribution from flexural bars could reach up to 77% of total applied shear force.
3. The flexural bar force development is also related to the shear reinforcement ratio as shear links rupturing could results in the load redistribution from links to flexural bars and cause the abrupt increase of bar force. With sufficient W-FRP shear reinforcement, the proposed model and actual testing which control the flexural bar strain to 0.7%, requiring no additional anchorage.
4. The prediction model shows good validity to predict the ultimate capacity, stiffness and development of tensile force in flexural bars.

Acknowledgement

The authors acknowledge and are grateful for the support of the BRE CICM (www.bath.ac.uk/bre), the University of Bath, EPSRC, China Scholarship Council and Weijiang Zhao Research Team at the Zhejiang University that has resulted in this work. Funding for experimental work from EPSRC grant EP/M020908/1 is acknowledged.

Reference

Bentz, E. C., Vecchio, F., and Collins, M. (2006). "Simplified modified compression field theory for calculating shear strength of reinforced concrete elements." *ACI Struct. J.*, 103(4), 614-624.

BSI (British Standards Institution) (2004). "Design of Concrete Structures: Part 1-1: General Rules and Rules for Buildings." *BS EN 1992-1-1:Eurocode 2*, London.

CSA (Canadian Standards Association) (2012). "Design and construction of building structures with fibre-reinforced polymers." *CSA S806-12*, Ontario, Canada.

Orr, J. (2012). "Flexible formwork for concrete structures." PhD, University of Bath.

Paglietti, A., and Carta, G. (2009). "Remarks on the Current Theory of Shear Strength of Variable Depth Beams." *The Open Civil Engineering Journal*, 3(1), 28-33.

Spadea, S., Orr, J., Nanni, A., and Yang, Y. (2017). "Wound FRP shear reinforcement for concrete structures." *Journal of Composites for Construction*, 21(5), 04017026.

Vecchio, F. J., and Collins, M. P. (1986). "The modified compression-field theory for reinforced concrete elements subjected to shear." *ACI Journal Proceedings*, 83(2).

Veenendaal, D., West, M., and Block, P. (2011). "History and overview of fabric formwork: using fabrics for concrete casting." *Structural Concrete*, 12(3), 164-177.

Yang, Y., Orr, J., Ibell, T., and Spadea, S. "Structural performance of flexibly formed concrete T beams with wound FRP reinforcement." *Proc., 8th Biennial Conference on Advanced Composites in Construction*, NetComposites Ltd, 283-288.

Yang, Y., Orr, J., and Spadea, S. (2018). "Shear Behavior of Variable-Depth Concrete Beams with Wound Fiber–Reinforced Polymer Shear Reinforcement." *Journal of Composites for Construction*, 22(6), 04018058.